Available on CMS information server

CMS NOTE 2006/125

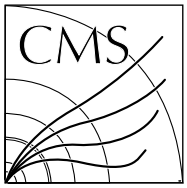

The Compact Muon Solenoid Experiment

CMS Note

Mailing address: CMS CERN, CH-1211 GENEVA 23, Switzerland

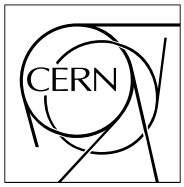

29th June 2006

Observability of the heavy neutral SUSY Higgs bosons decaying into neutralinos

C. Charlot [a)], R. Salerno [a) b)], Y. Sirois [a)]

a) Laboratoire Leprince-Ringuet, Ecole Polytechnique and IN2P3-CNRS, Palaiseau, France

b) Università di Milano Bicocca and INFN Milano, Milano, Italy

Abstract

A prospective study for the observability of heavy neutral Higgs bosons decaying into supersymmetric particles at the Large Hadron Collider is presented. The analysis focuses on the decay of the Higgs bosons into a pair of next-to-lightest neutralinos χ_2^0, followed by the cascade down to the lightest neutralino, $\chi_2^0 \rightarrow l^+l^-\chi_1^0$. The final state is characterized by the presence of four isolated leptons and missing transverse energy. The parameter space of the minimal Supergravity model is explored and favorable regions for the observation of the A^0/H^0 bosons are identified. The A^0/H^0 bosons could be discovered in the 2e2μ channel in the mass region $250 \lesssim m_{A/H} \lesssim 400$ GeV/c^2 with an integrated luminosity of 30 fb^{-1}.

1 Introduction

While the electroweak symmetry breaking via the Higgs mechanism in the Standard Model (SM) results in the existence of one physical neutral Higgs boson, supersymmetric (SUSY) theories require an extended Higgs sector. The Minimal Supersymmetric Standard Model (MSSM) for instance involves five physical states: a light CP-even (h^0), a heavy CP-even (H^0), a heavy CP-odd (A^0) and two charged Higgs bosons ($H^{\pm}$). Therefore, if SUSY particles are discovered at the Large Hadron Collider (LHC), the discovery of heavy neutral Higgs bosons would nevertheless be a major breakthrough in establishing the structure of the theory. Existing measurements yield as lower bounds 91.0 (91.9) GeV/c^2 for the h^0 (A^0) Higgs bosons of the MSSM [1].

The most promising channel to investigate the heavy Higgs sector of a SUSY theory is the $A^0/H^0 \rightarrow \tau\tau$ channel [2]. The $A^0/H^0 \rightarrow \mu\mu$ channel, although with a small branching ratio, offers the interesting possibility of allowing for a precise reconstruction of the Higgs boson mass. These channels have been shown to cover large parts of the intermediate and high tanβ region of the MSSM parameter space for an integrated luminosity of 30 fb^{-1} [2]. In these studies, the heavy Higsses decay into SM particles as it is assumed that sparticles are too heavy to participate in the decay processes.

The situation where, on the contrary, the decay of the heavy Higgs boson to sparticles is kinematically allowed has been recently investigated in CMS [3]. This is motivated by the fact that the existence of light neutralinos (χ^0), charginos ($\chi^{\pm}$) and sleptons ($\widetilde{l}$) is favoured by a large number of supersymmetric models in order to explain electroweak symmetry breaking without a large fine-tuning [4]. Also recent experimental results (precision measurements at LEP2 [1], muon $g-2$ [5]) may point towards the existence of light gauginos and sleptons.

Higgs bosons decaying into sparticles might therefore open possibilities to explore regions of the parameter space otherwise inaccessible via SM-like decays into ordinary particles [3] [6]. This is the case in particular in the difficult low and intermediate tanβ region of the MSSM parameter space. One of the most promising channels is the A^0/H^0 decay into a pair of next-to-lightest neutralinos, χ_2^0, followed by the leptonic decay $\chi_2^0 \rightarrow l^+l^-\chi_1^0$ (with $l = e, \mu$). This process results in a clean four lepton plus missing transverse energy ($\not\!\!E_T$) final state signature:

$$A^0/H^0 \rightarrow \chi_2^0\chi_2^0 \rightarrow 4l^{\pm} + \not\!\!E_T \ (l = e, \mu).$$

Since the phenomenological implications of SUSY are model-dependent, the discovery potential in given experimental conditions has to be studied resorting to some particular model, preferably with a limited number of free parameters. This implies some loss of generality, but ensures tractable predictions. In the minimal Supergravity model (mSUGRA), only four parameters and one sign, in addition to the SM parameters, need to be specified: the universal scalar m_0 and gaugino $m_{1/2}$ masses, the SUSY breaking universal trilinear coupling A_0, the ratio of the vacuum expectation values of the Higgs fields tanβ and the sign of the Higgsino mass parameter sign(μ).

The CMS detector has been described elsewhere [7]. In Section 2 of this note, the mSUGRA parameter space is scanned and three benchmark points are defined. Backgrounds are discussed in Section 3. The event simulation and online selection are described in Section 4 and the analysis cuts are presented in Section 5, focusing on the 2e2μ decay channel. The results obtained for the three benchmark points are shown in Section 6. Finally, the results are extrapolated to the whole parameter space and the CMS discovery reach for this decay channel is presented in Section 7.

2 Signal production

The purpose of this section is to determine the region of the mSUGRA parameter space where the decay chain of A^0/H^0 into four leptons have a sizeable cross-section times branching ratio. A scan of the $(m_0, m_{1/2})$ parameter plane for tan$\beta = 5, 10$ and sign(μ) = + is performed. Such values for tanβ are motivated by the fact that this region is not accessible for the $A^0/H^0 \rightarrow \tau\tau$ channel [2]. It has been checked that the branching ratios are rather insensitive to the sign of the Higgsino mass parameter μ, so that the results are also valid for the negative case. Finally, A_0 enters only marginally in the interpretation of the experimental results at the electroweak (EW) scale and is set to 0 throughout this study.

The signal cross-sections are computed using the HIGLU [8] and HQQ [9] programs. The branching ratios are evaluated using ISAJET [10] (version 7.69).

2.1 Production cross-section

For tan$\beta \gtrsim 5$, the radiation of a Higgs boson from bottom quarks ($q\bar{q}/gg \rightarrow A^0/H^0 b\bar{b}$) is the dominant production process for Higgs bosons in the MSSM, due to the larger couplings to $\mathrm{b\bar{b}}$. This is contrast to situation at very low tanβ (e.g. tan$\beta \simeq 2$), where the production is dominated by gluon fusion process ($gg \rightarrow A^0/H^0$)

mediated by SM-like top and bottom quark loops with additional contributions, in the case of the scalar CP-even Higgs boson (H^0), from stop and sbottom squark loops. Figure 1 presents the production cross-sections of the CP-even and CP-odd Higgs bosons. The two dominant production processes are shown for tan$\beta = 5$ and tan$\beta = 10$.

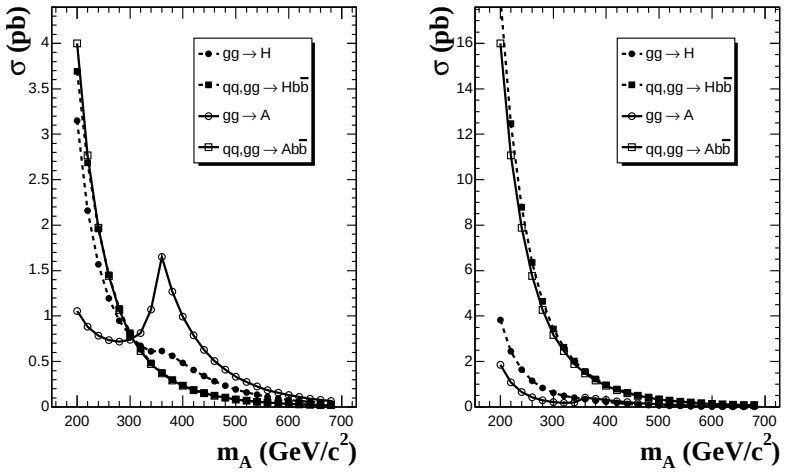

Figure 1: Production cross-sections of the heavy neutral Higgs bosons for the two dominant production processes $gg \rightarrow A^0/H^0$ (dotted lines) and $q\bar{q}/gg \rightarrow A^0/H^0 b\bar{b}$ (solid lines) for (left) tan$\beta = 5$ and (right) tan$\beta = 10$.

2.2 Decay of the heavy Higgs bosons into next-to-lightest neutralinos

Figure 2 shows the branching ratios of A^0 and H^0 decays into next-to-lightest neutralinos in the $(m_0, m_{1/2})$ parameter plane for tan$\beta = 10$, sign(μ) = + and $A_0 = 0$. Also indicated on Fig. 2 is the region forbidden for the theory, where no electroweak symmetry breaking is allowed, and the region excluded from cosmological constraints which require a neutral lightest supersymmetric particle. The 95% C.L. limit on the chargino mass obtained from searches at the LEP collider is also shown. The drop in branching ratio beyond $m_{1/2} \backsim 250$ GeV/c^2 which corresponds to $m_A > 350$ GeV/c^2 is due to the opening of the $t\bar{t}$ decay mode. The branching ratio of the CP-odd Higgs decay into next-to-lightest neutralinos is substantially higher than for the CP-even case. This is due to the fact that for the CP-even Higgs the couplings to SM particles are larger, thus leading to a larger total decay width and smaller branching ratios left over for decays into sparticles.

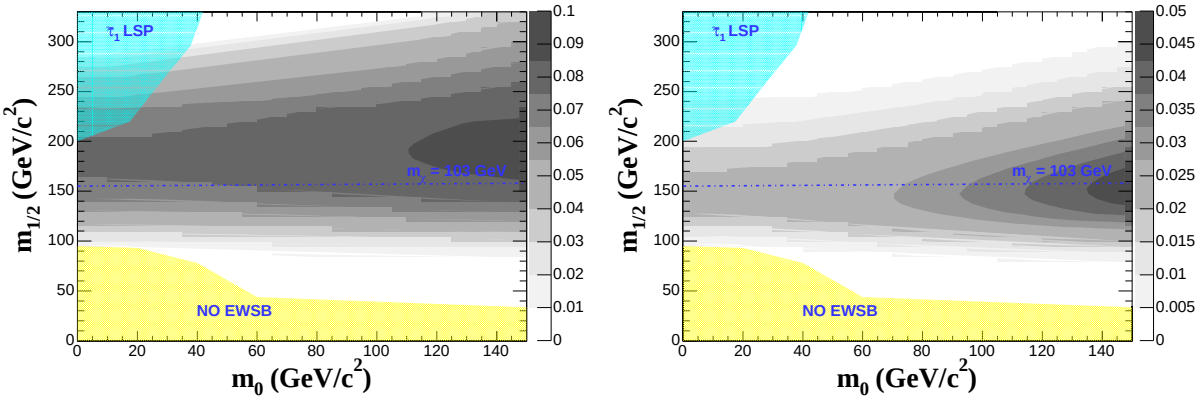

Figure 2: Branching ratio of the (left) A^0 and (right) H^0 decays into next-to-lightest neutralinos in the $(m_0, m_{1/2})$ parameter plane for tan$\beta = 10$, sign(μ) = + and $A_0 = 0$. The theoretically and experimentally excluded regions are indicated, as well as the LEP limit on the chargino mass (dashed-dotted line).

2.3 Decays of the next-to-lightest neutralino into leptons

The next-to-lightest neutralino decays into two fermions and a lightest neutralino: $\chi_2^0 \rightarrow f\bar{f}\chi_1^0$. The fermions are most often quarks, leading to two jets and missing E_T in the final state. To focus on a clean signature, the case where the neutralino decays into two leptons $\chi_2^0 \rightarrow l^+l^-\chi_1^0$, where $l = e$ or μ is considered here. If the sleptons are heavier than the χ_2^0, and provided that direct decays into a Z boson are not allowed (or are suppressed), only three-body decays $\chi_2^0 \rightarrow l^+l^-\chi_1^0$ contribute. These decays are mediated by virtual slepton or Z exchange. The corresponding branching ratios are presented in Figure 3. It is observed that, for the three-body decays, the branching ratios are sizable in the region $m_{1/2} \gtrsim 75$ GeV/c^2, $m_0 \gtrsim 55$ GeV/c^2 and $m_{1/2} \lesssim 2m_0$. If sleptons are lighter than the χ_2^0, direct two-body decays of the neutralino into a slepton-lepton pair are allowed. In mSUGRA the left and right-handed charged sleptons are not degenerated in mass and the two allowed regions for a χ_2^0 two-body decay are complementary. The branching ratios for such case are presented in Figure 4. The two-body decay branching ratios are significant only in a corner of the parameter space in the case of decay involving a left-handed slepton, and in the region $m_{1/2} \gtrsim 130$ GeV/c^2 and $m_{1/2} \gtrsim 2m_0$ in the case of a right handed slepton. Beyond $m_{1/2} \simeq 250$ GeV/c^2 the decays of the next-to-lightest neutralino to slepton-lepton pairs are suppressed due to the opening of the $\chi_2^0 \rightarrow \chi_1^0 h$ and $\chi_2^0 \rightarrow \chi_1^0 Z$ decay channels, in particular for m_0 values above $\simeq 150$ GeV/c^2.

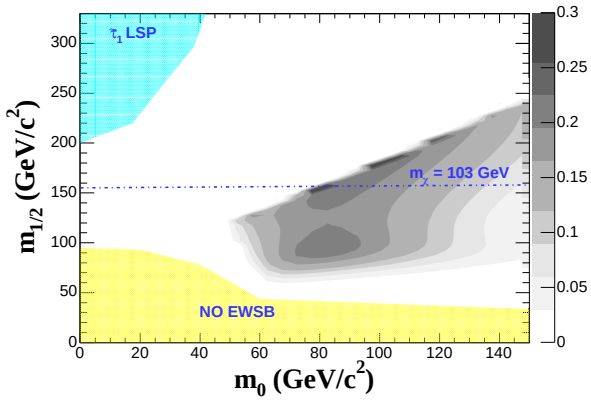

Figure 3: Branching ratio of the χ_2^0 three body decay $\chi_2^0 \rightarrow l^+l^-\chi_1^0$ in the $(m_0, m_{1/2})$ parameter plane and for tan$\beta = 10$, sign(μ) = + and $A_0 = 0$.

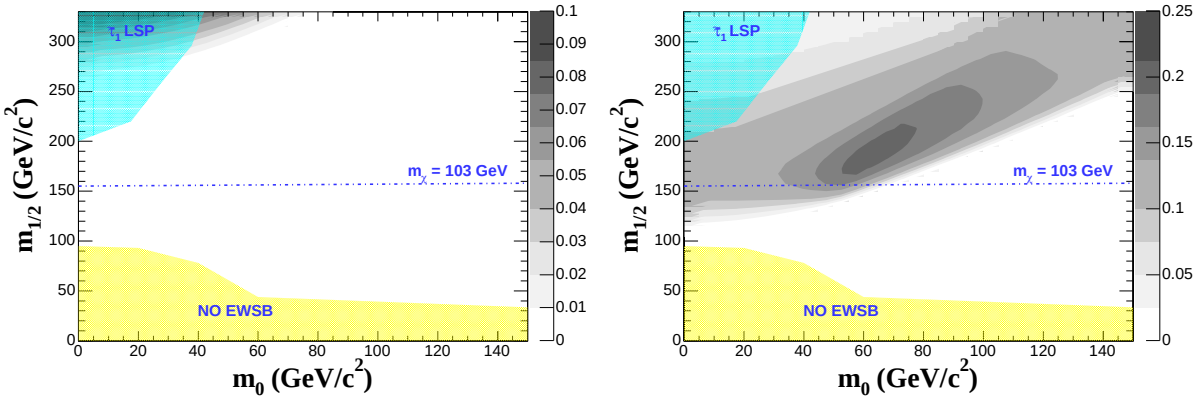

Figure 4: Branching ratio of the χ_2^0 two body decays (left) $\chi_2^0 \rightarrow \tilde{l}_L l$ and (right) $\chi_2^0 \rightarrow \tilde{l}_R l$ in the $(m_0, m_{1/2})$ parameter plane and for tan$\beta = 10$, sign(μ) = + and $A_0 = 0$.

2.4 Benchmark points

Figure 5 shows the production rate per fb^{-1} for the final state signature $A^0/H^0 \rightarrow 4l^{\pm} + \not{E}_T$ $(l = e, \mu)$ in the $(m_0, m_{1/2})$ plane for fixed $A_0 = 0$, sign(μ) = + and for tan$\beta = 5, 10$. Three benchmark points (A,B,C) are defined for the evaluation of CMS sensitivity whose corresponding mSUGRA parameters and mass of the involved

particles are presented in Tables 1 and 2. All these points have the following general features: a light right-handed slepton, implying that the direct two-body decay of the neutralino into a slepton-lepton pair is allowed, and light squarks and gluinos. The point C is the closest to the experimental limit on the chargino mass. It is also the most challenging one due to the huge SUSY background and the presence of very soft leptons in the final state coming from the small mass difference between the χ_2^0 and the $\widetilde{l}_R$.

Figure 6 shows the transverse momentum of the four leptons in the Higgs signal events for the points A, B and C (after the generator pre-selection cuts defined in Section 4). From now on, the analysis focuses on the particular 2e2μ decay channel which benefits from a twice as large event rate as for the 4e or 4μ cases.

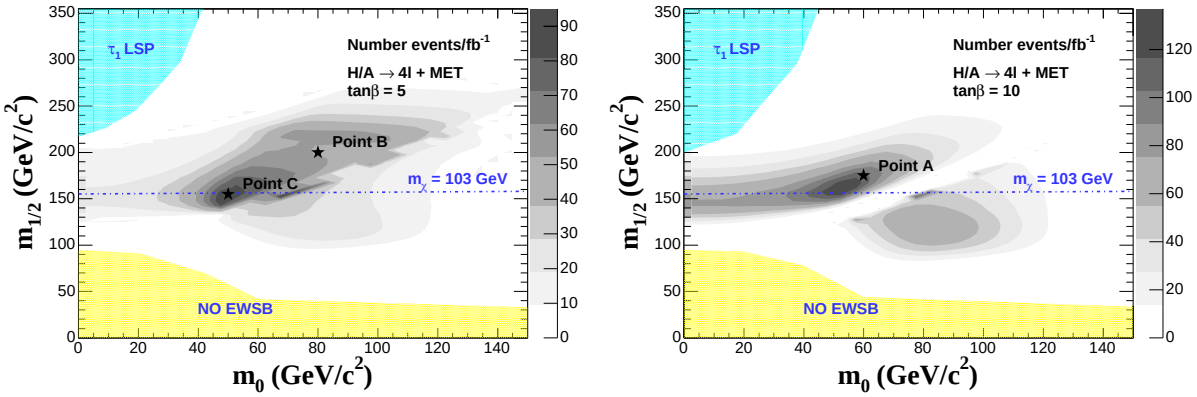

Figure 5: Event production rates for the final state signature $A^0/H^0 \rightarrow 4l^{\pm} + \not{E}_T$ $(l = e, \mu)$ in the $(m_0, m_{1/2})$ parameter plane for fixed $A_0 = 0$, sign(μ) = + and for (left) tan$\beta = 5$ and (right) tan$\beta = 10$. The three chosen benchmark points are indicated.

Point	m_0 (GeV/c^2)	$m_{1/2}$ (GeV/c^2)	A_0	tanβ	sign(μ)
A	60	175	0	10	+
B	80	200	0	5	+
C	50	150	0	5	+

Table 1: mSUGRA parameters for the three benchmark points.

Point	m_A	m_h	$m_{\chi_1^{\pm}}$	$m_{\chi 0_2}$	$m_{\chi 0_1}$	$m_{\tilde{l}_R}$	$m_{\tilde{l}_L}$	$m_{\tilde{g}}$	$m_{\tilde{t}_1}$
A	266	110	116	117	64	106	143	443	291
B	325	107	136	137	73	117	166	500	327
C	240	103	104	105	50	101	124	385	254

Table 2: Mass of relevant particles for the three benchmark points. Values are in GeV/c^2.

3 Background processes

There are two main categories of backgrounds to the considered signal: the SUSY and the SM backgrounds. In the SUSY category the dominant source of background is the production of leptons from the decays of squarks and gluinos which cascade to charginos and neutralinos. Unlike the neutralinos from the Higgs boson decay, the leptons in this case are produced in association with quarks and gluons. Therefore, the associated large hadronic activity can be used to suppress this type of background. An additional but smaller source of background comes from the direct production of slepton or gaugino pairs via the Drell-Yan processes and the direct production of χ_2^0 pairs. The rejection of these backgrounds is more difficult, as the hadronic activity in these events is very small. In the Standard Model category, three processes which yield to the same signature of four leptons in the final state contribute as backgrounds: $ZZ^{(*)}/\gamma^*$, $Zb\bar{b}$ and $t\bar{t}$. The potential background contribution from $Zc\bar{c}$ is expected to be negligible. Figure 7 shows the transverse momentum of the four leptons sorted in decreasing order for the different background processes.

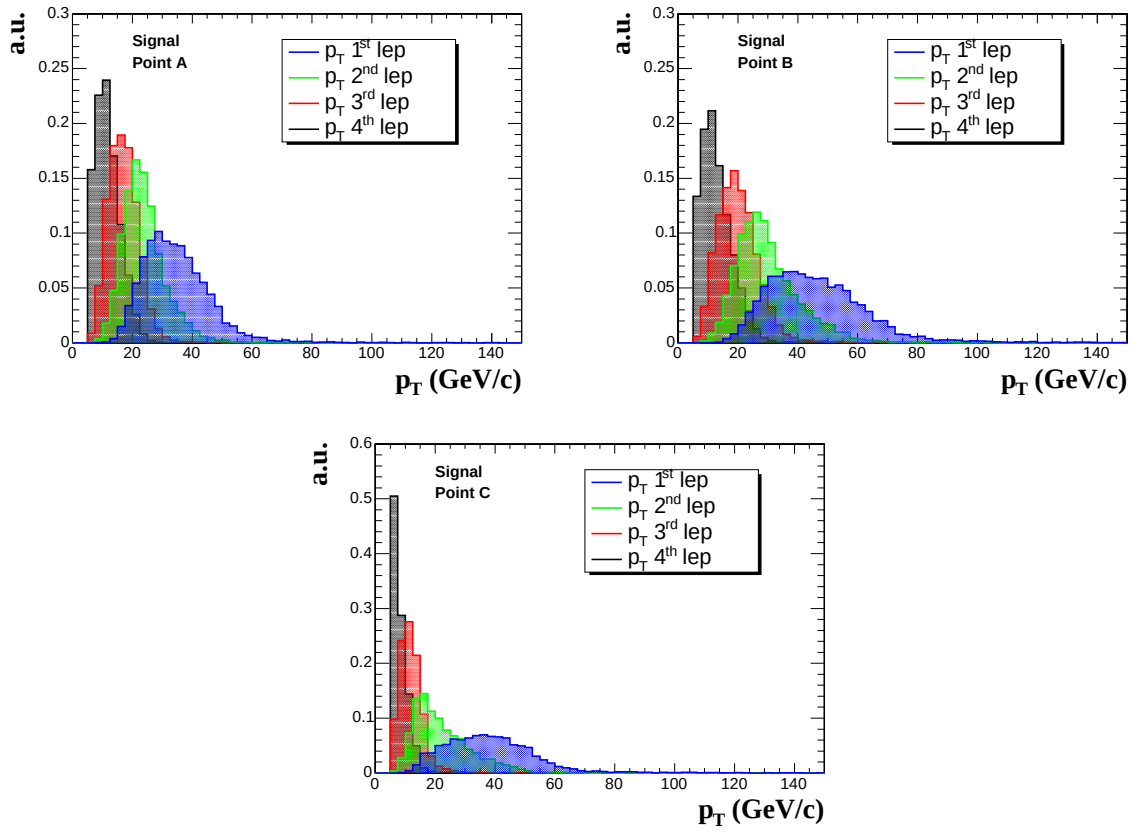

Figure 6: Transverse momentum distributions of the four leptons sorted in decreasing order for the Higgs signal and for the three benchmark points A (top, left), B (top, right) and C (bottom).

4 Event simulation and online selection

ISAJET [10] (version 7.69) and PYTHIA [11] (version 6.225) are used to generate the SUSY mass spectrum, to simulate events and the hadronisation and fragmentation to final state particles for the signal and the SUSY background. PYTHIA is used for the simulation of the SM backgrounds, together with CompHEP [12] for the case of the $\mathrm{Zb\bar{b}}$ background. The parton density functions (PDFs) in the proton are taken from the so-called CTEQ5 distributions. The signal cross-sections are computed using HIGLU and HQQ whereas the SUSY background cross-section is evaluated using PROSPINO [13]. In the SM backgrounds, the Z bosons (W bosons in the case of the $\mathrm{t\bar{t}}$ backgrounds events) are forced to decay to electrons or muons or taus, and in the case of decay to taus, the taus are subsequently forced to decay to electrons or muons. A pre-selection at generator level is applied, requiring an $\mathrm{e^+e^-\mu^+\mu^-}$ final state with p_T^{e} $(p_T^{\mu}) > 5$ (3) GeV/c and $|\eta| < 2.5$.

The CMS detector response is simulated using FAMOS [14] (version 1.4.0) with the effects of the low luminosity pile-up included. The off-line reconstruction of electrons and muons is performed using standard FAMOS algorithms. A muon candidate is defined as a track extending from the central tracking system to the outer muon system, and an electron candidate is defined as a supercluster in the electromagnetic calorimeter (ECAL) with an associated track.

A first and compulsory condition for the events is to satisfy the CMS Level-1 (hardware) trigger conditions and the filtering of the software High Level Trigger (HLT) [15]. For the two electrons and two muons case, it is found that taking the logical "OR" of the di-muon and di-electron triggers yields a high signal efficiency while suppressing the rate for the SM largest background, namely $\mathrm{t\bar{t}}$. The use of single electron and single muon triggers does not improve the final significance. Tables 3 and 4 summarize the Level-1 and HLT efficiencies for the signal and for the background processes with respect to the generator pre-selection. The global trigger efficiency is above 95% for the signal at point A and B. It is significantly lower (79%) for the point C due to the very soft leptons spectra arising from the smaller mass difference between the next-to-lightest neutralino and the right-handed slepton in this case.

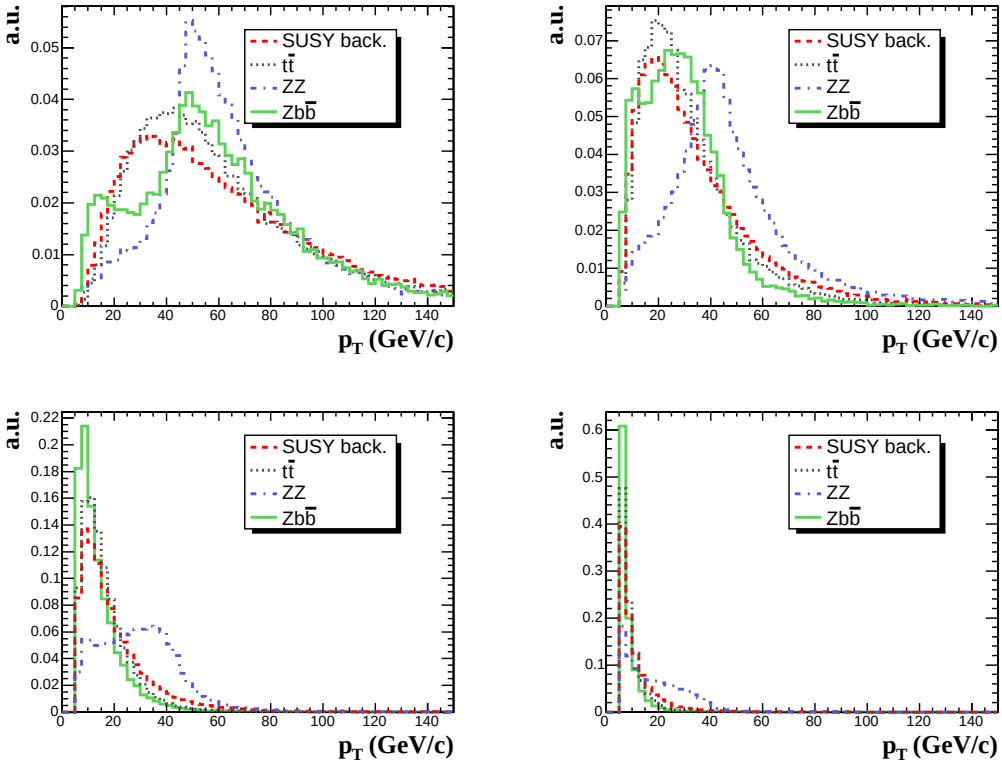

Figure 7: Transverse momentum distributions for each of the four leptons, sorted for each event in decreasing p_T^l order, for the different backgrounds to heavy neutral Higgs bosons and for the three benchmark points (top, left) A, (top, right) B, and (bottom) C.

Requirement for leptons (matching Level-1/HLT settings)			Efficiency (%) after generator pre-selection		
			Point A	Point B	Point C
$2e\,2\mu$ channel	**I**	2μ candidates ($E_T > 7$ GeV)	94	95	76
	II	$2e$ candidates ($E_T > 14.5$ GeV)	47	57	13
	I OR **II**		**97**	**98**	**79**

Table 3: Level-1 and High Level Trigger efficiency for the Higgs signal in the 2e2μ decay channel and for the three benchmark points. Both contributions of the di-electron and of the di-muon triggers are indicated.

	SUSY Back A	SUSY Back B	SUSY Back C	$t\bar{t}$	$Zb\bar{b}$	$ZZ^{(*)}/\gamma^*$
Level-1/HLT efficiency (%)	90	95	90	88	86	98

Table 4: Level-1 and High Level Trigger efficiency for each of the SUSY and SM background processes.

5 Signal versus background discrimination

The first step in the off-line event selection is to require that four leptons are reconstructed with the further requirement that the p_T of the electrons (muons) has a minimum value of 7 (5) GeV/c. The efficiency to reconstruct $e^+e^-\mu^+\mu^-$ events using off-line algorithms is given for the Higgs boson signal in Table 5.

5.1 Jet Veto

As already mentioned in Section 3, the large hadronic activity associated with the SUSY background can be used to suppress this type of process. A jet veto is also very efficient to suppress the $t\bar{t}$ and the $Zb\bar{b}$ backgrounds, due to the presence of jets in the final states for both of these background sources.

Jets are reconstructed from the electromagnetic (ECAL) and hadronic (HCAL) calorimeter towers using the

	Point A	Point B	Point C
$e^+e^-\mu^+\mu^-$ reconstruction efficiency (%)	80	81	72

Table 5: 2e2μ off-line reconstruction efficiency with respect to HLT for each of the three signal benchmark points.

iterative cone algorithm [16]. A cone radius of $R = 0.5$ and a seed tower threshold of $E_T = 1$ GeV are used. The jet veto consists in rejecting events with at least one reconstructed jet satisfying $E_T > 25$ GeV. A small fraction of signal events is found to be suppressed by the jet veto due to the presence of jets from pile-up events. The sensitivity of the analysis on the signal loss coming from 'fake' jets from pile-up is expected to be small and is not taken into account in this analysis. Figure 8 (left) shows the distribution of the hardest jet for the signal (point A) and for the background processes.

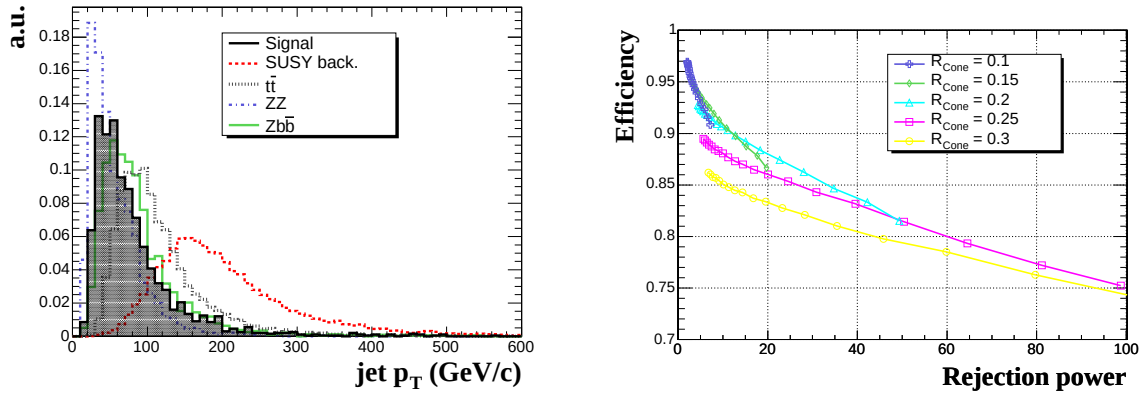

Figure 8: (left) distribution of the hardest jet for the signal (point A) and for the background processes; (right) isolation efficiency for the Higgs boson signal (point A) as a function of the rejection obtained against the $t\bar{t}$ background.

5.2 Lepton isolation

Track-based lepton isolation is used as the main tool to get rid of the $t\bar{t}$ and $Zb\bar{b}$ backgrounds. Reconstructed tracks are considered within an isolation cone in the (η, ϕ) plane of radius $R_{\rm cone} = \sqrt{\Delta\eta^2 + \Delta\phi^2}$ centred on each lepton. The tracks are required to have $p_T > 1.5$ GeV/c and $|\Delta\, IP_L| < 0.1$ cm, where $|\Delta\, IP_L|$ is the difference between the longitudinal impact parameter and the z position of the primary vertex. The lepton isolation variable is then defined as the sum of the p_T of all tracks satisfying these requirements but the lepton one, divided by the lepton p_T. The event isolation is finally defined as the requirement to have all the four leptons of the event isolated.

Figure 8 (right) presents the track based isolation efficiency for the signal (point A) after the generator pre-selection as a function of the rejection obtained against the $t\bar{t}$ background for different cone sizes. The cone size and the threshold are tuned to maximize the signal significance. In practice, a sufficient rejection power is obtained for a working point corresponding to an efficiency around 80%.

5.3 Missing transverse energy and 4-lepton transverse momentum

The SUSY background is characterized by a significant missing transverse energy ($\not\!\!E_T$) due to the presence of lightest neutralinos and of neutrinos produced from W and Z decays in the cascade decays of squarks and/or gluinos. The $\not\!\!E_T$ is reconstructed from the calorimeter towers (ECAL+HCAL) by adding vectorially the transverse energy measured in the calorimeter towers and the transverse energy of the reconstructed muons. Figure 9 shows the missing transverse energy for the Higgs signal (thick line) and for the backgrounds. Events are required to have $\not\!\!E_T <$ 80 GeV.

In addition, the correlation between $\not\!\!E_T$ and the 4-lepton transverse momentum (p_T^{llll}) in the case of the signal events is used. Events are selected if their distance to the axis $\not\!\!E_T = p_T^{llll}$ is less than 15 GeV. This selection is useful to further suppress the SUSY and $t\bar{t}$ backgrounds, as can bee seen on Figure 10 for the 2e2μ case.

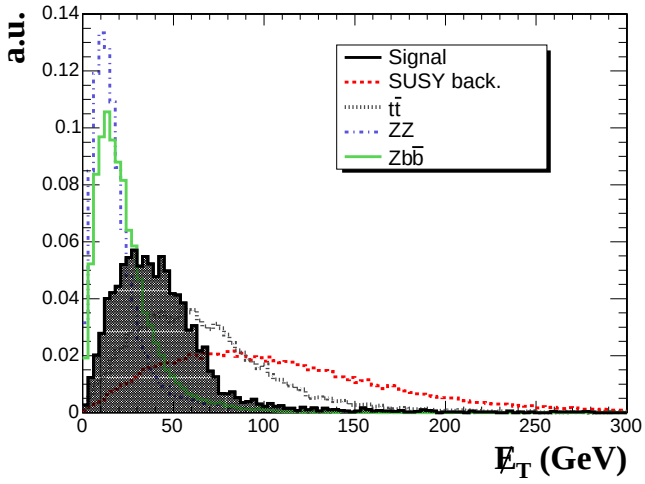

Figure 9: Missing transverse energy distributions for the signal (point A) and for the backgrounds.

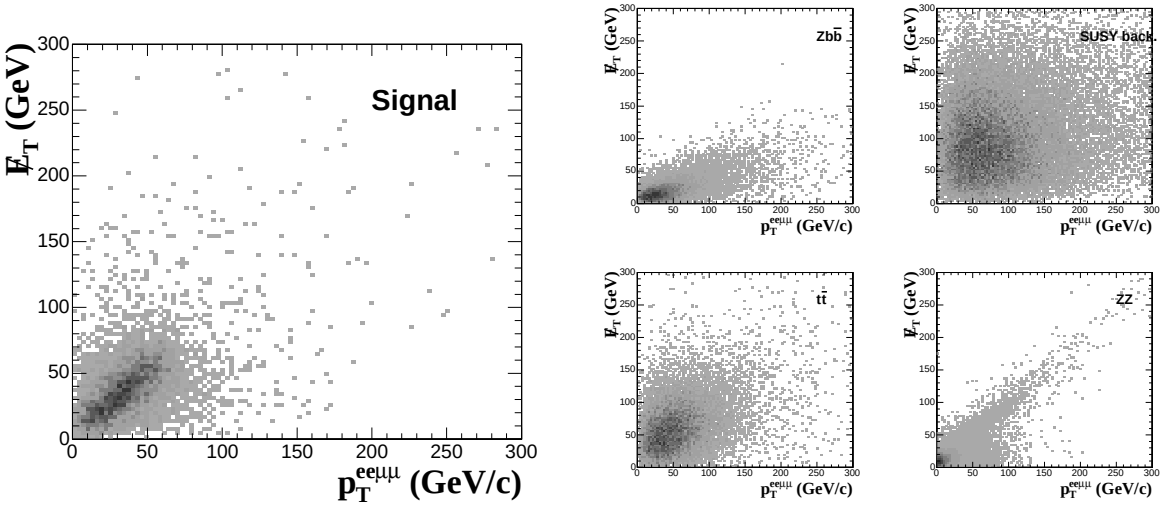

Figure 10: Correlation between the missing transverse energy and the 4-lepton transverse momentum: (left) for the Higgs signal (point A) and (right) for the background processes.

5.4 Invariant mass cuts

In order to suppress the backgrounds arising from SM $ZZ^{(*)}/\gamma^*$ and $Zb\bar{b}$ production, where at least one of the dilepton pairs is coming from a real Z boson, all events with a dilepton pair of opposite sign and same flavour leptons and satisfying $\mid m_{ll} - m_Z \mid < 10$ GeV/c^2 are rejected (Z veto). In addition, a minimum invariant mass of 12 GeV/c^2 is required on each dilepton pair in order to remove the contamination of bottomed and charmed mesons (Υ, J/Ψ, ...). Figure 11 presents the reconstructed di-lepton invariant mass distributions for the signal and for the different backgrounds.

An extra feature that can be exploited in the signal versus background discrimination is the shape of the dilepton invariant mass spectrum, which present a characteristic kinematical edge in the case of signal events. Since there are two χ_2^0's present in the Higgs decay, a double kinematical edge is visible in the particular case of the 2e2μ decay channel if one selects only events containing two electrons and two muons and then plots the di-electron invariant mass versus the di-muon invariant mass. The kinematical endpoint is near the mass difference between the χ_2^0 and χ_1^0, or if sleptons are intermediate in mass as is the case for the chosen benchmark points, near $\sqrt{(m^2_{\chi_2^0} - m^2_{\tilde{l}})(m^2_{\tilde{l}} - m^2_{\chi_1^0})}/m_{\tilde{l}}$. These distributions are shown for the three signal points and for the backgrounds in Figures 12 and 13 .

If not already discovered, the observation of such a kinematical edge would be a striking indication of super-

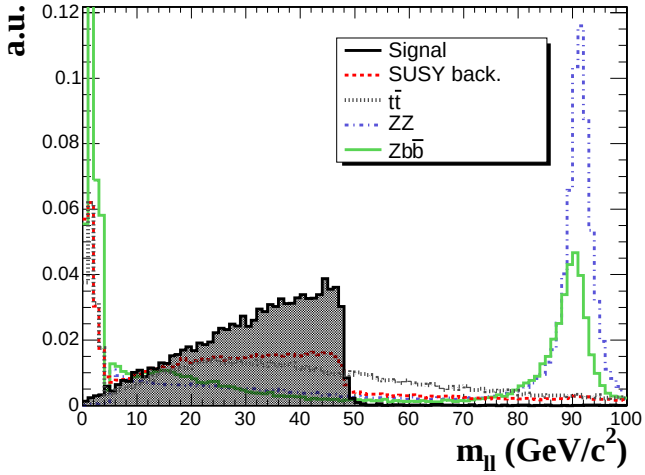

Figure 11: Reconstructed invariant mass of the di-muon and di-electron pairs for the signal (point A) and for the backgrounds.

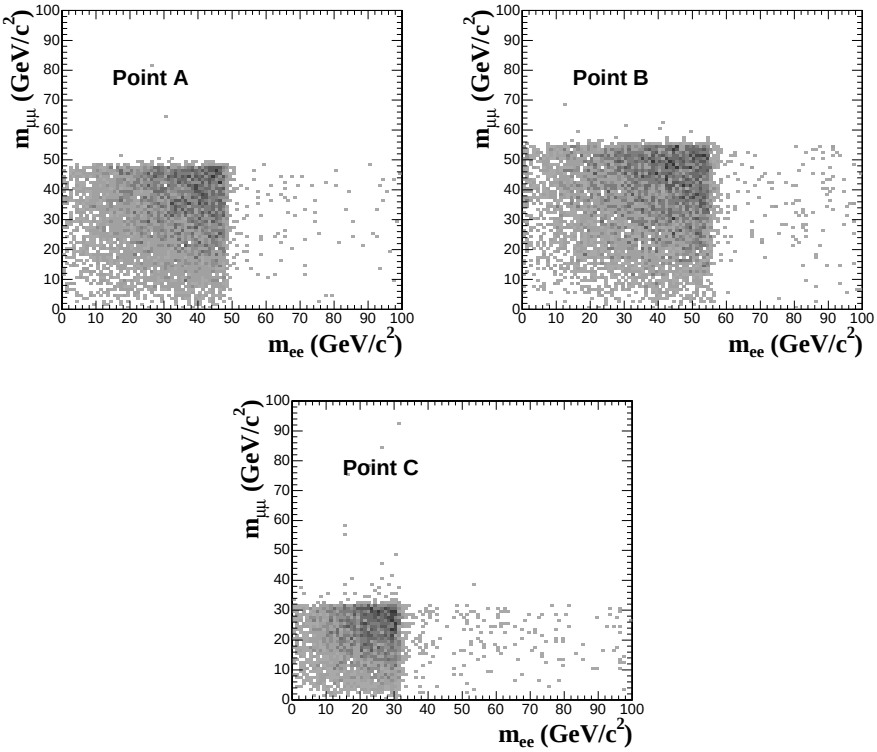

Figure 12: Double kinematical edge in the di-muon versus di-electron invariant mass distribution for the signal for the three benchmark points.

symmetry. Conversely, an 'a priori' knowledge of the mass difference between the next-to-lightest and the lightest neutralinos, in the case where SUSY would have been already discovered through squarks, gluinos, or sleptons, could help to separate a heavy neutral Higgs signal from the backgrounds. In the region of the parameter space relevant for this study, a loose cut in the mass difference at 65 GeV/c^2 is suitable for all Higgs mass values and is therefore used here as a starting value. An estimation of the mass difference from the discovery of other SUSY particles could be further used to improve the significance of the heavy neutral SUSY signal in a further refinement of the analysis.

Finally, a loose Higgs mass window cut is applied, also suitable for all relevant values of the parameter space.

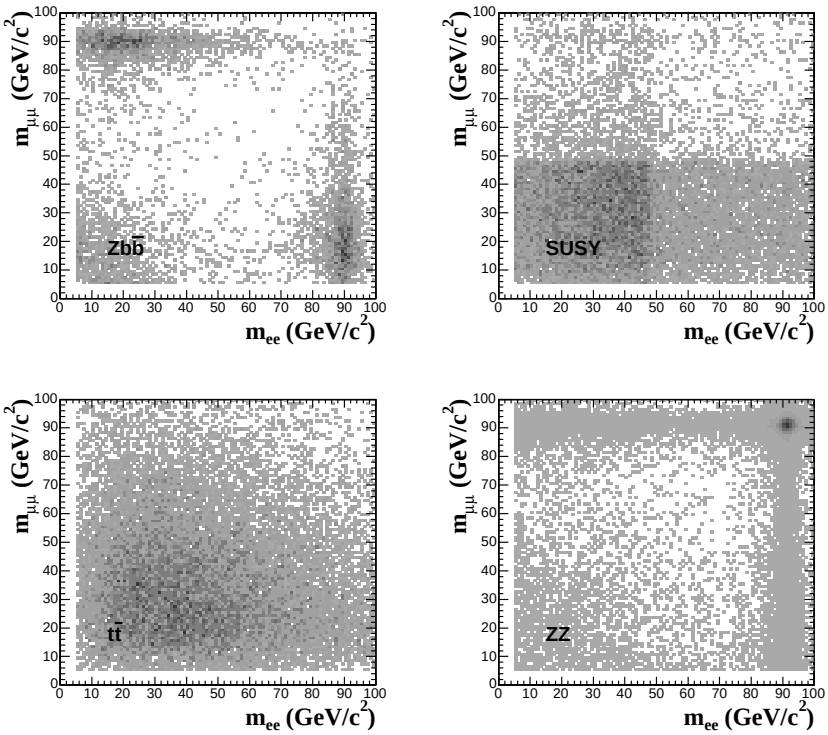

Figure 13: Double kinematical edge in the di-muon versus di-electron invariant mass distribution for the background processes.

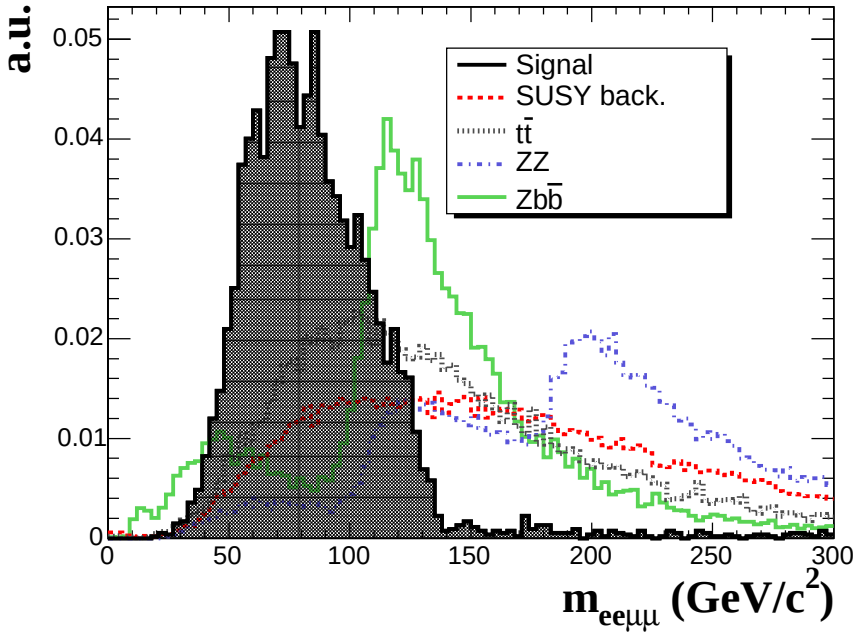

Figure 14: Distribution of the reconstructed invariant mass $M_{ee\mu\mu}$ for the Higgs boson signal (point A) and for the backgrounds.

Events are required to have a reconstructed 4-lepton invariant mass within 20 GeV/c^2 $< m_{llll} <$ 180 GeV/c^2. Figure 14 presents the 4-lepton invariant mass distributions for the signal and the backgrounds and for the 2e2μ specific case.

6 Results for the three benchmark points

Tables 6 and 7 summarize the production cross-sections and the cross-sections after each step of the online and off-line event selection, for the Higgs signal and for the SUSY and SM backgrounds. The efficiency of each cut with respect to the previous one is indicated in brackets. The cross-sections are given in fb and efficiencies are in percent. The global signal acceptances with respect to the production cross-section times branching ratio are 6.3%, 5.1% and 2.5% respectively for point A, B and C, whereas the acceptances for the SUSY backgrounds are 1.5×10^{-6}, 3.6×10^{-6} and 2.6×10^{-6} respectively, relative to the total SUSY production cross-section.

Figure 15 presents the reconstructed 4-leptons invariant mass distributions for each of the three benchmarks

	Point A fb (%)	Point B fb (%)	Point C fb (%)
σ	13.7 10^3	2.73 10^3	6.3 10^3
$\sigma \times B.R.$	108 (0.8)	54.5 (2)	65.9 (1.1)
$\sigma \times B.R. \times \epsilon$	33.4 (31)	18 (33)	13.1 (20)
Level-1/HLT	32 (97)	17.6 (98)	10.3 (79)
$e^+e^-\mu^+\mu^-$ reconstruction	25.5 (80)	14.2 (81)	7.4 (72)
Jet veto	8.2 (32)	3.5 (25)	1.9 (26)
Isolation cut	7.8 (97)	3.4 (96)	1.8 (94)
$\not{E}_T$& p_T^{lll} cuts	7.4 (94)	3.0 (89)	1.7 (95)
Z veto & min. dilepton mass	6.8 (92)	2.8 (95)	1.3 (75)
Dilepton edges cuts	6.8 (100)	2.8 (100)	1.3 (100)
Higgs mass window cut	6.8 (100)	2.8 (100)	1.3 (99)

Table 6: Production cross-sections and cross-sections after each step of the online and off-line selection for the Higgs signal and for the three benchmark points. Efficiencies with respect to the previous cut are quoted in brackets.

	SUSY Back A fb (%)	SUSY Back B fb (%)	SUSY Back C fb (%)	$t\bar{t}$ fb (%)	$Zb\bar{b}$ fb (%)	$ZZ^{(*)}/\gamma^*$ fb (%)
σ	216 10^3	116 10^3	430 10^3	840 10^3	278 10^3	29 10^3
$\sigma \times B.R.$	-	-	-	53.9 10^3 (63)	18.6 10^3 (6.7)	368 (1.27)
$\sigma \times B.R. \times \epsilon$	517 (0.2)	586 (0.5)	2020 (0.47)	682 (1.3)	258 (1.4)	33.7 (9.2)
Level-1/HLT	467 (90)	556 (95)	1824 (90)	600 (88)	221 (86)	31.2 (98)
$e^+e^-\mu^+\mu^-$ reconstruction	335 (72)	430 (77)	1346 (74)	274 (46)	132 (60)	23.1 (74)
Jet veto	2.0 (0.6)	3.0 (0.7)	7.6 (0.6)	6.6 (2.4)	6.9 (5.2)	10 (44)
Isolation cut	1.3 (62)	2.2 (72)	3.7 (48)	0.59 (9)	3.4 (50)	9.9 (98)
$\not{E}_T$& p_T^{lll} cuts	0.8 (63)	1.2 (54)	2.3 (62)	0.37 (64)	3.1 (92)	9.5 (95)
Z veto & min. dilepton mass	0.6 (76)	0.98 (83)	1.7 (73)	0.27 (71)	0.28 (9)	0.71 (7.5)
Dilepton edges cuts	0.40 (66)	0.74 (76)	1.36 (73)	0.12 (47)	0.17 (59)	0.37 (53)
Higgs mass window cut	0.34 (85)	0.43 (57)	1.1 (80)	0.11 (86)	0.17 (100)	0.36 (96)

Table 7: Production cross-sections and cross-sections after each step of the online and off-line selection for the various backgrounds. Efficiencies with respect to the previous cut are quoted in brackets.

points after the selection. Results are given for an integrated luminosity of 30 fb^{-1}. Each background contribution is added to the previous one (histograms) and finally to the Higgs signal (points). The statistical significance is then estimated forming the test of the hypothesis of signal plus background against the background only hypothesis using a likelihood ratio (LLR). Assuming Poisson statistics, the counting log-likelihood significance is then defined as:

$$S_{cL} = \sqrt{2((N_s + N_b)\ln(1 + N_s/N_b) - N_s)} \quad (1)$$

Table 8 gives, for the points A,B and C, the statistical significances as obtained from the log-likehood ratio and counting events in the range $20 < m_{ee\mu\mu} < 180$ GeV/c^2, after all selection cuts and for an integrated luminosity of 30 fb^{-1}. As a result, the A^0/H^0 could be easily discovered at the points A and B with such an integrated luminosity, while for the point C the signal visibility is lower due to the higher SUSY background in this case.

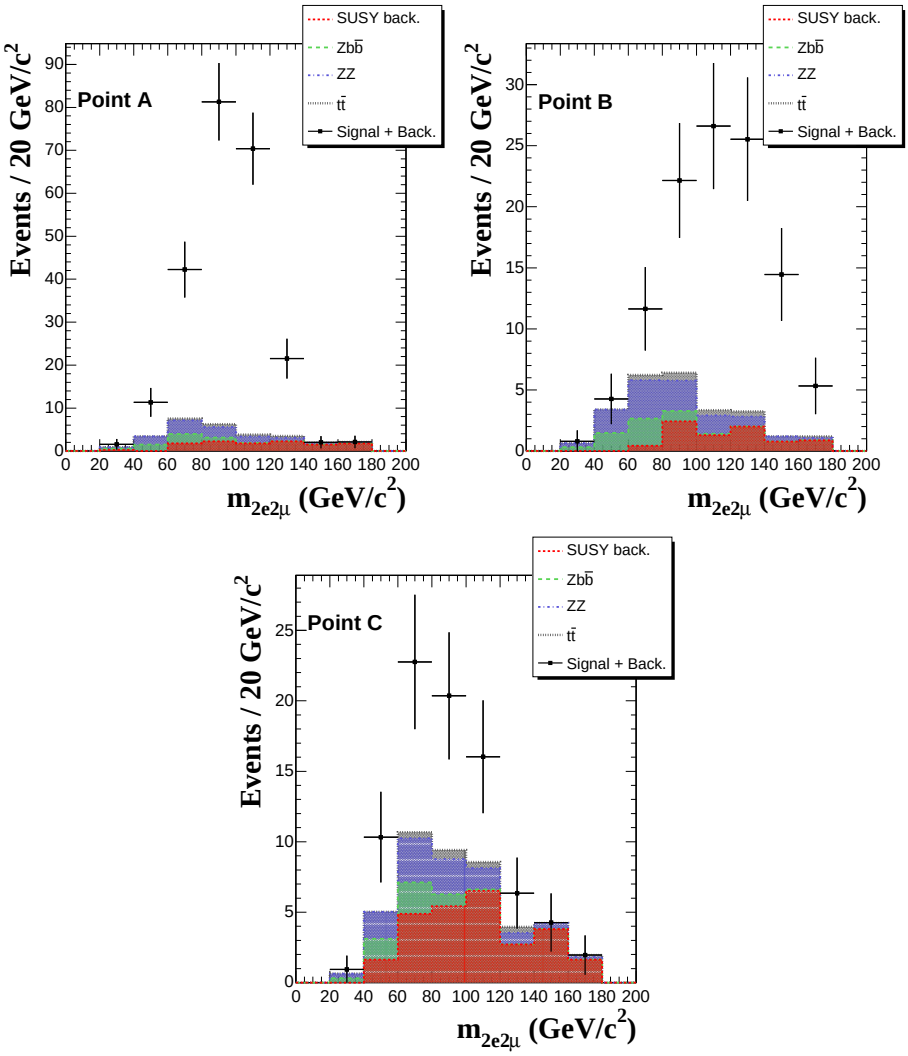

Figure 15: Four lepton invariant mass distributions for the three benchmark points: (top, left) point A, (top, right) point B and (bottom) point C. Each background contribution is added to the previous one (histograms) and finally to the Higgs signal (points). Results are given for an integrated luminosity of 30 fb^{-1}.

	Point A	Point B	Point C
S_{cL}	23.6	11.5	4.8

Table 8: Statistical significance for the three benchmark points counting events in the range $20 < m_{ee\mu\mu} < 180$ GeV/c^2, after all selection cuts and for an integrated luminosity of 30 fb^{-1}.

7 CMS discovery potential

A calculation of the CMS 5σ discovery reach is performed, extrapolating the results obtained for the three benchmark points. To determine the reach in the $(m_0, m_{1/2})$ parameter plane, the calculation of the signal $\sigma \times B.R.$ at each point of the $(m_0, m_{1/2})$ plane is used (Fig. 5). The signal selection efficiency is parametrized as a function of the pre-selection efficiency determined for each point of the plane, using the fact that this pre-selection efficiency is directly related to the leptons p_T spectra and approximating the signal selection efficiency to a pure p_T dependence effect. The number of SUSY background events is evaluated using for each point in the plane the total SUSY production cross-section and taking as the background acceptance the highest value among the ones obtained for the three representative points after the selection (conservative approach). For the SM backgrounds, the final cross-sections after all selection cuts as given in Table 7 are used. Finally, the significance for an integrated luminosity of 30 fb^{-1} is computed taking into account an estimation of the systematic uncertainty on the number of background events.

The jet energy scale is expected be calibrated in CMS using photon plus jet events and an integrated luminosity of 10 fb^{-1}. Accordingly, a variation of the jet energy of 10% to 3% depending on the jet p_T is applied. Its effect on the background estimation is found to be of the order of 6%. The missing transverse energy is expected to be well measured and understood from single Z and single W production. The $\not\!\!E_T$ measurement can be controlled, e.g. via single Z production by artificially removing one lepton. Uncertainties of 4.5% for the $\not\!\!E_T$ resolution and of 2% for the $\not\!\!E_T$ scale are deduced from W mass measurement studies [17] and are applied. The resulting uncertainty on the background estimation is found to be of the order of 4%. Finally, a 5% uncertainty is taken as the systematic uncertainty on the background estimation from the luminosity measurement.

Figure 16 shows the extrapolated 5σ-discovery contours in the $(m_0, m_{1/2})$ plane, for an integrated luminosity of 30 fb^{-1}. The values of the other mSUGRA parameters are: $A_0 = 0$, sign(μ) = + and tan$\beta = 5, 10$.

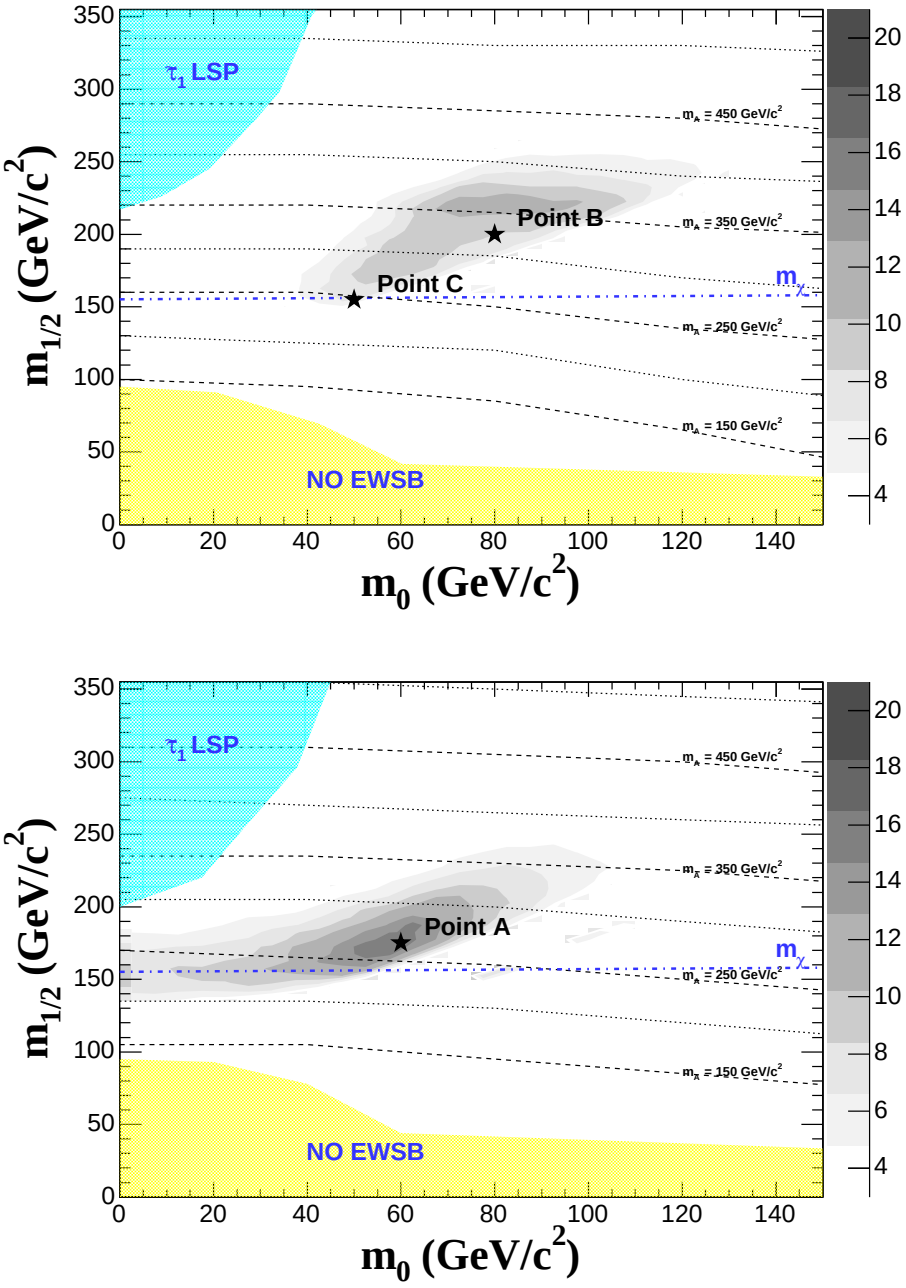

Figure 16: 5σ-discovery contours for $A^0/H^0 \to \chi_2^0\chi_2^0 \to 4l + \not\!\!E_T$ in the $(m_0, m_{1/2})$ plane for fixed $A_0 = 0$, sign(μ) = + and for (top) tan$\beta = 5$ and (bottom) tan$\beta = 10$. Iso-mass curves for the CP-even Higgs boson are indicated (dashed and dotted lines). The results are shown for an integrated luminosity of 30 fb^{-1}.

The complex structure of the discovery region is mainly determined by the cross-section times branching ratio of $A^0/H^0 \rightarrow \chi_2^0\chi_2^0 \rightarrow 4l + \not{E}_T$. The A^0/H^0 could be discovered through their decays to neutralino pairs in the region 150 GeV/$c^2 < m_{1/2} <$ 250 and 40 GeV/$c^2 < m_0 <$ 130 GeV/c^2 for tan$\beta = 5$ and in the region 140 GeV/c^2 $< m_{1/2} <$ 240 GeV/c^2 and $m_0 <$ 110 GeV/c^2 for tan$\beta = 10$. This corresponds to heavy neutral Higgs bosons masses in the range 250 GeV/$c^2 \lesssim m_{\mathrm{A,H}} \lesssim 400$ GeV/c^2, as can be seen from the iso-mass curves also indicated on the Fig. 16.

8 Conclusions

A prospective study for the observability of heavy neutral Higgs bosons decaying into two next-to-lightest neutralinos in CMS has been performed. The analysis focuses on the leptonic decay channel of the next-to-lightest neutralinos, $\chi_2^0 \rightarrow l^+l^-\chi_1^0$, thus leading to four isolated leptons plus missing transverse energy as the characteristic final state signature. The main backgrounds can be sufficiently suppressed using appropriate selection criteria. In particular, the important SUSY background which arises in the mSUGRA framework from the existence of light sleptons can be efficiently reduced using a jet veto, mass independent missing transverse energy and 4-lepton transverse momentum cuts, and exploiting also the correlation between these two kinematical variables in signal events. In the 2e2μ decay channel, the characteristic double kinematical edge in the dilepton invariant mass distributions can be further used to suppress the backgrounds. A starting value is used which could be further refined in a scenario where SUSY would have been already discovered through the observation of SUSY particles. It is shown that, depending on the selected point in the SUSY parameter space, the A^0 and H^0 Higgs bosons could be discovered in the 2e2μ decay channel in the mass region 250 GeV/$c^2 \lesssim m_{\mathrm{A,H}} \lesssim 400$ GeV/c^2 for an integrated luminosity of 30 fb^{-1} .

9 Acknowledgments

We wish to gratefully thank the PRS Higgs working group for the support. Special thanks to Filip Moortgat and Daniel Denegri for very helpful discussions. Many thanks also to Michael Schmitt for his very useful comments and editorial help during the finalization of the note.

References

[1] The LEP Working Group for Higgs searches, ALEPH, DELPHI, L3 and OPAL collaborations, Phys. Lett B365 (2003) 61.

[2] D. Denegri et al., Summary of the CMS Discovery Potential for the MSSM SUSY Higgses, CMS Note 2001/032.

[3] S. Abdullin D. Denegri and F. Moortgat, Observability of the heavy neutral SUSY Higgs bosons decaying into neutralinos, CMS Note 2001/042.

[4] M. Bastero-Gil, G. Kane and S. King, Phys. Rev. B474 (2000) 103-112.

[5] S. Komine et al., Phys. Rev. B506 (2001) 93-98.

[6] H. Baer and X. Tata, Phys. Rev. D47 (1993) 2739-2745.

[7] CMS collaboration, The Compact Muon Solenoid - Technical Proposal, CERN/LHCC 94-38.

[8] M. Spira, HIGLU: A program for the calculation of the total Higgs production cross-section at hadron colliders via gluon fusion including QCD corrections, hep-ph/9510347.

[9] M. Spira, http://mspira.home.cern.ch/mspira/proglist.html.

[10] F. E. Paige, S. D. Protopopescu, H. Baer and X. Tata, ISAJET 7.69: A Monte Carlo Event Generator for p p, anti-p p, and e+e- reactions, hep-ph/0001086.

[11] T. Sjostrand et al., Comput. Phys. Commun. 135 (2001) 238-259.

[12] E. Boos et al., CompHEP Collaboration, Nucl. Instrum. Meth. A534 (2004) 250-259.

[13] W. Beenakker, R. Hoepker and M. Spira, PROSPINO: A program for the production of supersymmetric particles in next-to-leading order QCD, hep-ph/9611232.

[14] http://cmsdoc.cern.ch/famos/.

[15] CMS collaboration, The trigger and Data Acquisition Project, CERN-LHCC 2000-038.

[16] CMS collaboration, CMS Physics Technical Design Report, Volume 1, CERN-LHCC 2006-001.

[17] V. Buge et al., Prospects for the Precision Measurement of the W Mass with the CMS Detector at the LHC, CMS Note 2006/061.